SAND99-0496C

Thermal Decomposition Characteristics of Orthorhombic Ammonium Perchlorate (*o*-AP) *

Leanna Minier and Richard Behrens †
Combustion Research Facility
Sandia National Laboratories
Livermore, CA 94551

ABSTRACT

Preliminary STMBMS and SEM results of the thermal decomposition of AP in the orthorhombic phase are presented. The overall decomposition is shown to be complex and controlled by both physical and chemical processes. The data show that the physical and chemical processes can be probed and characterized utilizing SEM and STMBMS. The overall decomposition is characterized by three distinguishing features: an induction period, and acceleratory period and a deceleratory period. The major decomposition event occurs in the subsurface of the AP particles and propagates towards the center of the particle with time. The amount of total decomposition is dependent upon particle size and increases from 23% for ~50μm-diameter AP to 33% for ~200μm-diameter AP. A conceptual model of the physical processes is presented. Insight into the chemical processes is provided by the gas formation rates that are measured for the gaseous products. To our knowledge, this is the first presentation of data showing that the chemical and physical decomposition processes can be identified from one another, probed and characterized at the level that is required to better understand the thermal decomposition behavior of AP. Future work is planned with the goal of obtaining data that can be used to develop a mathematical description for the thermal decomposition of *o*-AP.

INTRODUCTION

The propellant community maintains a great interest in understanding the combustive behavior of ammonium perchlorate (AP) owing to its widespread use as the oxidant in solid rocket propellants. The safety characteristics of rocket motors that utilize AP-based composite propellant are determined by the response of the propellant in abnormal environments associated with fire, impact, and/or shock. Understanding the response of AP in these environments is critical, since the propellant typically contains greater than 65% w/w (weight/weight) AP. The response of the solid propellant in a fire can be especially hazardous, since heating of the propellant can alter its chemical and physical characteristics. This altered state can result in combustive characteristics that are quite different from the normal propellant, and may lead to very rapid deflagration, explosion, and possibly transition to detonation. To address these safety issues requires understanding and characterizing both the thermal decomposition of the propellant prior to ignition and the combustive behavior of the chemically and physically altered propellant after ignition.

Although AP is used extensively in rocket propellant and has been the subject of a large number of investigations over the past 50 years, most of these investigations have focused on the combustion of AP, and only limited numbers of investigations on the decomposition of AP at lower temperatures (<500°C) are available. The studies at low temperatures were conducted in the 1950's and 1960's and are summarized by the work of several investigators.[1-6] This work has largely been ignored by the propellant community, as more recent efforts have focused on understanding the higher temperature combustive processes. However, to address the issues associated with safety and "slow cookoff," understanding these low temperature processes is important. The development of mathematical models to predict the response of propellants in fires requires a well-defined understanding of these low temperature processes, since they will control the ignition processes and the ensuing combustive event.

To extend the work of the previous investigators and to develop a better understanding of the processes that control the decomposition of AP at low temperatures (<500°C), we have conducted exploratory experiments on the thermal decomposition of AP in the cubic phase (> 240°C) and the thermal decomposition of an AP-based propellant. The results of the exploratory experiments have been reported at a previous JANNAF meeting.[7] That work showed that there are two main processes controlling the thermal decomposition of neat AP, an observation

---

* Approved for public release; distribution is unlimited.

† Work supported by a Memorandum of Understanding between the U.S. Department of Energy and the Office of Munitions. Sandia is a multiprogram laboratory operated by Sandia Corporation, a Lockheed Martin Company, for the United States Department of Energy under Contract DE-AC04-94AL85000.

DISCLAIMER

consistent with the literature cited previously. The two processes are commonly referred to as the low-temperature and high-temperature decomposition regimes, respectively. Jacobs and Russell-Jones presented a general reaction schematic (R1) to describe the two decomposition regimes that occur below 500°C; Step 2 represents a surface reaction that is said to dominate the low-temperature regime, and Step 5 represents the high-temperature regime that consists of gas-phase reactions.[8] Our work showed the following: 1) The low-temperature regime dominates at temperatures below ~270°C and occurs in the solid-phase, not on the surface of the AP. 2) The major products are H_2O, O_2, Cl_2, N_2O and HCl. 3) In this regime approximately 30% of the AP decomposes, leaving behind an agglomerate of fine, unreacted particles of AP. 4) The high-temperature regime dominates at temperatures above 300°C and involves the dissociative sublimation of AP to NH_3 and $HClO_4$, and subsequent extensive secondary reactions of NH_3 and $HClO_4$ in the gas-phase.

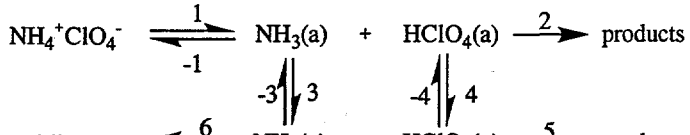

(R1)

The objective of our ongoing AP study is twofold. First, we intend to identify the physical and chemical processes that dominate the thermal decomposition behavior of AP in the orthorhombic (*o*-AP) and cubic phases, and understand how they are coupled to one another. The experimental conditions are chosen to examine the thermal decomposition behavior of AP utilizing the techniques of simultaneous thermogravimetric modulated beam mass spectrometry (STMBMS) and scanning electron microscopy (SEM). The STMBMS method is used to identify the gaseous decomposition products and determine their time-dependent behavior during the decomposition process. The SEMs provide detailed information on changes in morphology of the AP particles resulting from having undergone controlled extents of decomposition. Second, based on the experimental results, we will develop a model of the processes that control the decomposition of *o*-AP and the low-temperature regime.

We are currently obtaining a better understanding of the thermal decomposition processes of AP in the orthorhombic phase (*o*-AP). The chemical and physical decomposition processes are not well understood, although three major decomposition steps have been proposed for the physical processes: 1) nucleation of the reaction sites, 2) nuclei growth and coalescence to form an interface between reacted and unreacted AP, and 3) decomposition of the interface.[2,5,6] The description of the reaction sites has been described previously from hot stage and SEM results on single AP crystals.[5] These previous studies reveal that a greater depth of knowledge of the chemical and physical decomposition processes, and how they are coupled, must be obtained in order to construct a mathematical model that describes the decomposition event.

In this paper we present our preliminary results from the thermal decomposition of neat AP in the orthorhombic phase. The results include the identities of the gaseous decomposition products and the temporal behaviors of the product gases as they evolve, referred to as the gas formation rates (GFR), taken from STMBMS experiments. We present results on the morphological features of the AP particles observed from SEM images taken during different stages of the thermal decomposition. The results show that the physical and chemical decomposition processes are coupled, that particle size affects the decomposition process and that the pressure of the confined gaseous decomposition products, outside of the particle, slows the decomposition rate. The results show that new and insightful information has been obtained on the thermal decomposition processes of o-AP, which will provide the information required to develop a mathematical model of the thermal decomposition processes.

EXPERIMENTAL

INSTRUMENT DESCRIPTION

STMBMS. The STMBMS apparatus and basic data analysis procedure have been described previously.[9-11] This instrument allows the concentration and rate of formation of each gas-phase species in a reaction cell to be measured as a function of time by correlating the ion signals at different m/z values measured with a mass spectrometer with the force measured by a microbalance at any instant of time during the experiment. In the experimental procedure, a small sample (between 10 and 60 mg) is placed in an alumina reaction cell that is then mounted on a thermocouple probe that is seated in a microbalance. The reaction cell is enclosed in a high-vacuum environment ($<10^{-6}$ Torr) and

is radiatively heated by a bifilar-wound tungsten wire on an alumina tube. The molecules from the gaseous mixture in the reaction cell exit through a small diameter orifice (5μm, 25μm and 230μm in these experiments, orifice length is 25μm) in the cap of the reaction cell and traverses two beam-defining orifices before entering the electron-bombardment ionizer of the mass spectrometer where the ions are created by collisions of 20 eV electrons with the different molecules in the gas flow. A relatively low electron energy of 20 eV is used to reduce the extent of fragmentation of the higher molecular weight ions. The pressure of the gas within the reaction cell depends on the degree of confinement of the gaseous products. The maximum pressures range from less than 1 Torr for experiments with the larger diameter orifices (230μm) and lower confinement, to approximately 20 Torr for experiments with smaller diameter orifices (5μm) and higher confinement. Further details of the instrument can be obtained from the references.

STMBMS data analysis. The thermal decomposition data of AP has been analyzed using the general procedure described previously.[11] At the lower temperatures used in this study, sublimation of the AP was insignificant. Therefore, it was not necessary to correct for fragmentation of the AP sublimation products in the quantification procedure.

SEM. Scanning electron microscopy (SEM) is utilized in this study to correlate the physical appearance of the AP with the thermal decomposition data obtained with the STMBMS. The instrument used is a JEOL 840*f*. SEM images of whole particles, and particles cleaved with a clean razor blade are obtained. The AP particles are taken from a lot of AP with a nominal 200μm average particle diameter.

MATERIALS

The AP utilized in this study was obtained from NAWC, China Lake. Samples utilized in this study are from two different lots of AP, having nominal average particle diameters of 200μm and 20μm. The particle-size distribution of the two lots of AP are shown in Table 1. Both lots of AP contain approximately 0.1% tricalcium phosphate (TCP) as an anticaking agent.

EXPERIMENTAL CONDITIONS

The experimental conditions for the STMBMS thermal decomposition experiments that are used to determine the thermal decomposition characteristics and the effect of particle size, containment, and temperature on the thermal decomposition behavior are listed in Table 2.

Table 1. AP particle-size distribution.

Distribution for Nominal 200μm AP	% by weight	Distribution for Nominal 20μm AP	% by weight
425-599	0.5	>150	1.8
300-424	9.7	90-149	6.4
212-299	37.1	63-89	18.7
150-211	29.7	38-62	55.4
90-149	20.3	<38	17.7
63-89	2.4		
38-62	0.3		

Table 2. Experimental Parameters.

Experiment	Material	Particle diameter (μ)[1]	Temperature [2] (°C)	Sample size (mg)	Orifice Diameter (μ)
I	AP	200	190.7	10.0	25
II	AP	200	170.8	12.2	25
III	AP	200	179.9	12.9	25
IV	AP	200	229.3	10.1	25
V	AP	200	190.1	10.4	230
VI	AP	200	189.6	7.3	5
VII	AP	38-62	190.0	9.9	25
VIII	AP	155-211	189.8	10.7	25
IX	AP	425-599	191.7	9.3	25

[1] Nominal 200μm and 20μm diameter AP are used for experiments unless otherwise indicated.
[2] Temperature uncertainty is ±0.3°C.

MINIER

RESULTS AND DISCUSSION

The rate of decomposition of AP is controlled by both chemical and physical processes. The nature of the chemical processes are derived from both this work and information from the literature (basically summarized in R1). The physical processes also play an important role in the decomposition of AP, transforming the pristine, crystalline AP particle into a highly porous AP agglomerate, as illustrated in Figure 1. The underlying physical processes that lead to this transformation are: 1) Initial nucleation and growth of the reaction centers in a layer below the surface of the particle. 2) Propagation of this reactive layer away from the surface, consuming the core of the particle and leaving the agglomerate of AP behind. The thickness and propagation rate of the reactive layer into the particle is determined by the processes that control the nucleation and growth of the reaction center. 3) Growth of the reaction center is controlled by the generation of gaseous decomposition products within the reaction center and the mechanical strength of the solid AP in the reactive layer. 4) Reactions cease within the reactive layer when the mechanical strength of the solid AP in the reactive layer can no longer contain the gaseous decomposition products within the reaction centers. The increasing porosity within the reactive layer leads to a decrease in its mechanical strength.

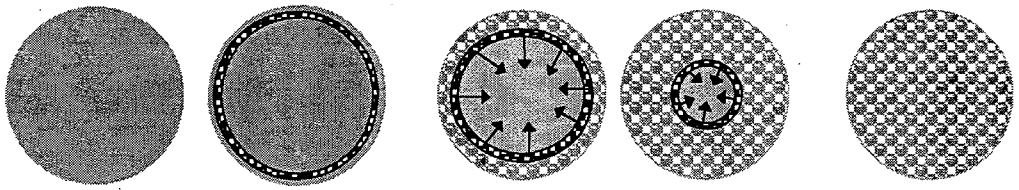

1. Pristine AP **2. Nucleation and Growth at subsurface** **3. Growth and Coalescence (shrinking of AP core)** **4. AP Agglomerate (solid-phase reaction)**

Figure 1. Conceptual model for the physical processes occurring during the thermal decomposition of AP in the orthorhombic phase (*o*-AP).

Insight into the nature of the chemical processes is developed through careful analysis of the temporal behaviors of the GFRs of the decomposition products. The temporal behaviors of the GFRs are characterized by an induction period, an acceleratory period and a deceleratory period. In the induction period very low levels of gaseous decomposition products are detected. The acceleratory period is characterized by increasing GFRs, ultimately reaching their maximum values. The deceleratory period is characterized by decreasing GFRs.

PHYSICAL PROCESSES

Comparison of the SEM images of pristine AP, and of AP particles that have been exposed for various lengths of time at 190°C, reveals differences in the morphology. SEMs of pristine and thermally damaged AP, shown in Figures 2-5, contain features that indicate the presence of nuclei and reaction centers. They also show the presence of an interface between two zones of differing morphology. One zone, in which AP decomposition has occurred, has a porous structure that is different from the morphology of the pristine AP. The other zone, in which decomposition has not occurred, shows little change in AP morphology. Similar features have been described by Kraeutle in his hot-stage and SEM studies.[12]

The pristine AP particles have a spheroidal geometry and contain internal, nonuniform structural defects in the form of voids and striations (Figure 2a). The higher magnification SEM (Figure 2b) reveals dark regions on the cleaved surface, which may be small voids. The SEM image of the cleaved face of an AP particle held at 190°C for 2 hours (Figures 3a and 3b) is compared to the image of pristine AP. As will be shown later, an AP particle maintained for two hours at 190°C has progressed approximately halfway through the induction period of decomposition process. The SEM image of the heated AP particle at 500x does not reveal any obvious differences from the morphology of the pristine AP. At 5000x, the surface of the cleaved AP particle appears to be pitted. The pits have diameters of ~ 0.5 μm, appear to be evenly distributed, and may be nucleation centers similar to those previously described by Kraeutle.

Figure 4 represents an AP particle that has been quenched during the very early stages of the decomposition process. The particle has lost ~3.6 weight percent of its original weight during the decomposition process. Figure

4a shows that the porous portion of AP is forming at the subsurface and at structural defects near the particle surface. An interface between a reacted and unreacted zone in the AP particle appears to be developing. Higher magnification images (Figures 4b and 4c) indicate that the large voids in the AP have distinct geometrical features and exist only in a limited volume beneath the surface of the particle. This volume appears to be a layer in which most of the decomposition occurs. This reactive layer is created initially below the surface of the particle and propagates towards the center of the AP particle as the decomposition process progresses. The SEMs shown in Figures 5a and 5b illustrate an end point of the propagation of the reactive layer. After being held at 190°C for 25 hours, the low-temperature decomposition process is complete, and the AP particle has been completely transformed to an agglomerate of fine AP particles, as illustrated schematically in Figure 1. Overall the changes in the morphology of *o*-AP, due to thermal decomposition, are consistent with our model of the physical processes described previously in Figure 1. The changes in morphology owing to decomposition are also consistent with Kraeutle's observations.[12]

CHEMICAL PROCESSES OF THE THERMAL DECOMPOSITION *o*-AP

The physical and chemical processes that control the decomposition of *o*-AP are coupled and complex. To unravel this complexity, the identities of the thermal decomposition products are determined and the temporal behaviors of the GFRs are measured as a function of temperature, containment of the gaseous products, and AP particle size.

General thermal decomposition characteristics. The general thermal decomposition behavior of AP in the orthorhombic phase is determined from the results of an experiment with 200-μm diameter AP, thermally decomposed at 191°C in a reaction cell fitted with a 25μm-diameter orifice (Experiment I; Table 2). The gaseous decomposition product identities, the time-dependent behavior of their GFRs and the resulting weight-loss profile are illustrated in Figure 6.

The weight-loss profile is characterized by a sigmoidal curve that exhibits five features; 1) an initial weight loss that occurs during the temperature ramp to isothermal conditions, 2) an induction period, 3) an acceleratory period, 4) a deceleratory period, and 5) a period where the rate of weight loss is small and continues to the termination of the experiment. The weight loss shows that approximately 33% of initial AP mass is lost during the experiment. The percent weight loss observed is consistent with that reported in the literature for the thermal decomposition of AP in the orthorhombic phase.[1,6,12]

The identities of the gaseous products and the time-dependent behavior of their respective GFRs reveal many interesting features of the decomposition process. The products of dissociative sublimation are characterized by the behaviors of NH_3 and $HClO_4$ during the pyrolysis. The major gaseous decomposition products are H_2O, O_2, Cl_2, HCl, and N_2O. Minor gaseous products include N_2, NO_2 and NO. Also observed but not included in Figure 6 are the trace products of HNO_3, HClO, and an ion signal at *m/z* 69. The species at *m/z* 69 is suspected to be H_2ClO_2 owing to the presence of an ion peak at *m/z* 71 (originating from the $H_2{}^{35}ClO_2$ species) that is temporally correlated and a third of the intensity of *m/z* 69.

The time-dependent behavior of the GFRs for the major gaseous products exhibited the following features. 1) Both H_2O and NH_3 evolve at the onset of heating and continue into the induction period. The absence of other decomposition products in substantial quantities during this time may indicate that the early presence of NH_3 and H_2O originate from a desorbtion process and not from a decomposition process. 2) The ratio of NH_3 and $HClO_4$ is not constant throughout the decomposition reaction, as would be expected for uninhibited sublimation (R1). This implies that processes other than dissociative sublimation contribute to the final amount of NH_3 and $HClO_4$ that is detected. 3) An induction period of substantial time is apparent during the experiment. 4) At the onset of decomposition, the GFRs of the decomposition products are temporally correlated, suggesting that there is one major decomposition regime. This contrasts to the two distinct sets of peaks observed for the nonisothermal decomposition of AP in the cubic phase that represented two distinct decomposition regimes.[7] 5) The GFRs of the products are fairly symmetrical about the maximum GFR obtained during the experiment. The shape of the curves provides information on the relationships between the rate of nucleation, growth and rupture of the reactive centers, the rate of propagation of the decomposition reaction, and the rate that the gaseous products evolve from the AP agglomerate into the reaction cell. 6) The GFRs for the less abundant products of HCl and $HClO_4$ show similar behaviors to one another in that they achieve their maximum GFRs prior to the major products. This is indicative

that another process occurs in addition to the process that results in the formation of the major products. 7) At the end of the decomposition event, the product GFRs do not go to zero but are continuously detected at a low level.

A high degree of coupling exists between the chemical and physical processes and is best illustrated by the identities and temporal behaviors of the GFRs of the major products Cl_2, H_2O, O_2 and N_2O. These products appear simultaneously after an induction period of significant duration has elapsed. From the time of their appearance, the respective GFRs of these final products consistently track one another throughout the acceleratory and deceleratory periods of the decomposition process. Such behavior almost suggests that a single chemical pathway leads to their formation. However, the nature of the decomposition products indicates that multiple and complex chemical reactions take place prior to the formation of the final products. The chemical decomposition reactions of AP that must occur to form Cl_2, H_2O, O_2 and N_2O clearly include the following: 1) consecutive reactions that involve the destruction and formation of several molecular bonds and 2) multiple reactive collisions that occur between reaction intermediates. Various global chemical decomposition reactions for AP at temperatures below 240°C have been reported to explain the formation of the major products.[1,13,14] The reactions indicate several steps are required to produce the final products and do not isolate the chemical processes from the physical processes. The observed highly correlated temporal behavior of the major products observed in this study can be reasonably explained by considering a strong coupling of the chemical processes to the physical processes.

The correlated temporal behavior of the GFRs of the major products (Cl_2, H_2O, N_2O and O_2) is due to the influence of the physical processes involving the growth and rupture of the reaction centers. The reaction center undergoes growth from gas-phase reactions and surface reactions that occur within the center. When the confinement of the reaction center is lost, the volatile decomposition products evolve. The simultaneous evolution of the gaseous products results in the observed correlated temporal behaviors of the GFRs.

The return to very low decomposition rates after the decay stage of the low-temperature channel indicates that the solid-phase reaction chemistry ceases when confinement is lost. The low-level GFRs after the end of the major decomposition event could be due to low-level reactions occurring on the surface of the remaining AP agglomerate.

The evolution of NH_3 and $HClO_4$ indicate that the dissociative sublimation process (R1; Steps 1 and –1) occurs simultaneously with the decomposition processes of *o*-AP. Based upon the values and time-dependent behavior of the GFRs for NH_3 and $HClO_4$, two general observations are made. Dissociative sublimation can be substantially suppressed during the decomposition of *o*-AP by conducting the reaction under slight confinement (a 25μm-diameter orifice is used in this experiment to provide partial confinement). This is evidenced by the lower GFRs of NH_3 and $HClO_4$ relative to those of the major decomposition products. Also, a mass balance reveals that the NH_3 and $HClO_4$ contribute less than 1% to the total mass loss (~33%) of AP during the low-temperature thermal decomposition process. Additionally, the GFR values of NH_3 and $HClO_4$ remain low after the low-temperature decomposition event ceases and the sublimation process becomes dominant.

The second observation is that processes other than dissociative sublimation control the time-dependent behavior of the GFRs of NH_3 and $HClO_4$. The GFRs for NH_3 and $HClO_4$ do not track one another during the induction period and during the major decomposition event. During the induction period the GFR of NH_3 appears, peaks and decays whereas the GFR for $HClO_4$ remains negligible. At the onset of the major decomposition event, the temporal behavior of the GFR for NH_3 is similar to those of the major decomposition products whereas the GFR for $HClO_4$ makes its appearance and then peaks prior to those of the major decomposition products. The simultaneous presence of H_2O with the NH_3 during the induction may reflect a correlation between the H_2O and NH_3. We are currently trying to identify the source of the H_2O that is observed during the induction period as to whether it originates from adsorbed H_2O or from an early decomposition pathway.

The appearance of the GFR of $HClO_4$, HCl and N_2 at the onset of decomposition and their subsequent growth and peaking prior to those of the main decomposition products is an interesting feature that we are currently evaluating in greater detail. The differing temporal behaviors of these products relative to the major decomposition products clearly indicates that the decomposition of AP involves multiple processes. It is not clear at this time if the source of $HClO_4$ originates from an enrichment process or from a decomposition reaction. A decomposition event is occurring that involves the decomposition of AP and appears to be correlated to the presence of $HClO_4$. This additional decomposition event involves the formation of minor gaseous product N_2. The early peaking of these minor products may be related to the early growth and development of the reaction centers. Work is currently being conducted to better characterize this other process.

Effect of temperature on orthorhombic AP thermal decomposition. Experiments to evaluate the effect of temperature on the isothermal decomposition of *o*-AP were conducted with 200μm-diameter AP particles at 171°, 180°, 191°and 229°C (Experiments I, II, III and IV; Table 2). An orifice diameter of 25μm on the reaction cell is utilized in these experiments to minimize the dissociative sublimation process in the temperature range being examined. The weight loss data from all four temperatures is included in this report. Evaluation of the trends observed in the GFRs are illustrated by data collected from experiments at 171°C and 191°C.

The temperature effect on the weight-loss behavior is illustrated in Figure 7. The weight loss curves for the decomposition experiments at 171°, 180° and 191°C are similar and suggest that similar physical processes occur at these temperatures. An induction period is observed that decreases with increasing temperature, and the characteristic sigmoidal shape of the weight loss curve is retained. The approximate fraction of weight lost due to the major decomposition event is consistently between 30 and 34%. The exception is the weight-loss curve obtained from the decomposition of AP at 229°C where approximately 38% of the weight is lost. Our data does show that a continued low level of weight loss is observed after the major decomposition event ceases. Further data is currently being collected between 190° and 240°C to probe the decomposition trend that occurs as the decomposition temperatures approach the phase-transition temperature. This data will be used to evaluate the effect of temperature on the induction period and on the decomposition processes.

The major products and the general time dependence of their respective GFRs are observed to be similar to one another at 171° and 191°C as is shown in Figure 8. Differences in the ratios of the GFRs between the various products are observed. For example, a trend exists showing that the time-dependent behavior of the GFR of NH_3 decreases with increasing temperature relative to that of the $HClO_4$. The decomposition products show slight changes in some of the relative ratios. For example, the ratio between H_2O and O_2 decreases from approximately 2 to 1.5 as the temperature is increased from at 171° to 191°C. A change in the ratio as a function of temperature is also observed between the GFRs of Cl_2 and N_2O and the GFRs of Cl_2 to O_2. The temperature dependence of the ratios will be better assessed from the data collected in the decomposition experiments conducted between 190° and 240°C.

Effect of containment of gaseous products on orthorhombic AP decomposition. The effect of changing the pressure of the gaseous decomposition products confined in the reaction cell on the decomposition behavior of 200μm-diameter AP was examined on AP at ~190°C by utilizing orifice diameters of 5μm, 25μm and 230μm (Experiments I, V and VI; Table 2). The resulting weight-loss profiles are presented in Figure 9. The resulting GFRs of the main products, their temporal behaviors, and the pressures of the main products formed in the reaction cell are presented in Figure 9.

Although the sigmoidal features of the three weight loss curves are similar, higher confinement of the gaseous products resulted in decreasing the rate of weight loss. The weight loss behaviors of the two less-confined experiments are similar. A pronounced difference is observed at the highest level of containment of the decomposition products; the acceleratory period is extended and the rate of the deceleratory period is decreased. The pressure curves for the main products at 191°C (bottom of Figure 10) show that the maximum pressures in the reaction cells fit with the 230μm, 25μm and 5μm-diameter orifices are approximately 0.015, 0.7 and 18 Torr, respectively. The increase in the measured pressure between the 230μm and 25μm-diameter orifice experiments is about a factor of 47 and the increase between the 25μm and 5μm-diameter experiments is about a factor of 30. The decomposition process appears to be sensitive to the effect of increased containment of the reaction products within the reaction cell. This affect could arise from several processes. An evaluation of the product identities and their time-dependent behavior is required to obtain any insight into the effect of containment.

The comparison of the decomposition products and their GFRs, shown in Figure 10, reveal several interesting features of the decomposition process. 1) The containment of the decomposition gases does not affect the induction period and product identities. This observation is consistent with the decomposition reactions occurring in the solid phase of the AP. 2) The GFRs of the sublimation products are influenced by confinement. At maximum confinement, the GFR of NH_3 is enhanced and no $HClO_4$ is observed. 3) The width of the GFR curves (duration of the decomposition event) is broadened and the GFRs are less than those of the less-confined experiments. 4) The ratio between H_2O and O_2 remains similar with confinement. 5) The GFR of HCl is enhanced with increased confinement. 6) The ratio of Cl_2 to O_2 decreases with confinement. 7) The temporal behaviors of $HClO_4$ and HCl show an inverse relationship; as the pressure inside the reaction cell increases, the GFR of $HClO_4$ decreases and the GFR of HCl increases. This relationship suggests that a direct relationship between HCl and $HClO_4$ exists.

The effect of high confinement on the time-dependent behavior of the GFRs is quite pronounced. The symmetry of the GFRs for the experiments utilizing the 230 and 25μm-diameter orifices is similar both in the magnitude of the GFRs and the overall time-dependent shape of the GFR curves. At the highest confinement (5μm-diameter orifice) the overall symmetry of the GFRs about the maximum GFR is maintained despite the maximum GFR being increased in time by a factor of 1.5 relative to the less-confined experiments. Close examination of the acceleratory portion of the GFR curves at highest confinement reveals a shoulder in the curve at approximately 30000 seconds (easier to observe with the GFR of NH_3). The GFRs then accelerate from the shoulder to their maximum value at about 50000 seconds. The shoulder correlates in time with the maximum GFR values obtained in the less-confined experiments and may be representative of the early decomposition process when pressure exerts less of an effect on the reactions.

The observation that increased confinement had an affect on the decomposition reaction indicates that processes other than the decomposition reaction within the reaction center occur. These other processes must be better understood as they can have a strong influence on the overall decomposition behavior of *o*-AP with circumstances that involve high pressures or containment. The current insight obtained from the presented data will be useful in our ongoing effort to unravel the thermal decomposition processes of *o*-AP.

Effect of particle size on thermal decomposition of orthorhombic AP. The effect of particle size on the decomposition was examined in experiments conducted at 190°C, utilizing three different particle size distributions: 38-62μm, 150-211μm and 425-599μm. A 25μm-diameter orifice is used in the reaction cells to reduce the contribution of AP sublimation to the overall decomposition process. The weight loss results and temporal behaviors of the GFRs resulting from these experiments (VII, VIII and IX; Table 2) are shown in Figures 11 and 12.

The comparison of the weight-loss behaviors (Figure 11) reveals four notable features. (1) The general features of the decomposition process in the solid phase are the same as previously described. (2) The onset of the acceleratory weight-loss period is not affected by the particle size. (3) The weight loss rates that are observed for the two larger particle sizes are similar, with the larger particle exhibiting a slightly faster decomposition rate during the acceleratory period. In contrast, the small diameter AP particles lose weight at a substantially slower rate. (4) The total amount of weight lost increases with particle size. The large and medium particle AP show an approximate 33% weight loss from decomposition and the small particles shows an approximate 23% weight loss. The lesser percent weight loss observed for the smaller particle, relative to the middle-sized particles, is consistent with a subsurface reaction occurring for the reasons described in our previous work.[7] The similar weight loss observed for the ~200μm and ~500μm-diameter AP is interesting. One possible explanation for the similar weight losses is that the larger particles of the AP are not single particles but are conglomerates of smaller particles. An examination of a few-milligram sample of the ~500μm-diameter AP sample under a light microscope at the time this paper was being written revealed that conglomerates did make up some of the AP particles of the sample being examined.

The decomposition product identities and the behavior of the GFRs of the major decomposition products show the same general behavior that has been observed throughout this study for the thermal decomposition of *o*-AP (Figure 12). Comparisons of the time-dependent behavior of the GFRs is revealing despite the uncertainty of the particle size of the ~500μm-diameter AP. In general, the temporal behaviors of the show similar behaviors but with the following differences: 1) The smallest particle size produces lower GFRs than the larger particles. The width of its peak is longer in time than the larger particles reflecting a slower decomposition time. 2) The temporal behaviors of HCl and $HClO_4$ are very different from the other products. A sharp increase in the maximum GRF of HCl occurs during the acceleratory period for the experiments using the ~200μm and ~50μm diameter particles. This observation is consistent with previous results that suggest the $HClO_4$ and HCl are products resulting from surface or condensed phase reactions and are closely associated with the early nucleation and growth of the reaction centers.

The features of the decomposition behavior of the ~50μm and ~200μm-diameter AP are consistent with the physical decomposition scheme presented in Figure 1. A smaller fraction of decomposition is expected with the smaller particle size due to the smaller volume available in the subsurface of the smaller particles. Comparative interpretations involving the GFRs for the ~500μm-diameter AP are not reasonable to make at this time due to the uncertainty of the actual average particle size making up the ~500μm-diameter AP. Further work is being conducted in this area.

SUMMARY

In this paper we present our preliminary STMBMS and SEM results on the thermal decomposition of *o*-AP, which provide new insights into the nature of the decomposition processes at low temperatures (<500°C). The STMBMS method is used to identify the gaseous decomposition products and determine their time-dependent behavior during the decomposition process. The SEMs provide detailed information on changes in morphology of the AP particles resulting from having undergone controlled amounts of decomposition. This information will be used to develop a model of the processes that control the decomposition of AP-based composite propellants, which can be used to characterize the state of a propellant prior to ignition. A combination of this information and the combustion characteristics of the degraded propellants will be used to develop engineering models needed to predict the response of propellants in abnormal environments, such as fire.

The thermal decomposition behavior of *o*-AP is complex and involves both chemical and physical processes. The two processes can be probed and studied in detail by using data obtained with the SEM and STMBMS techniques.

A conceptual model of the physical processes that characterize the decomposition of *o*-AP has been developed. 1) The nucleation and growth of the reaction centers begin in a layer below the surface of the particle. 2) This reactive layer propagates away from the surface, consuming the core of the particle and leaving the agglomerate of AP behind. 3) The thickness and propagation rate of the reactive layer into the particle is determined by the processes that control the nucleation and growth of the reaction center. 4) Growth of the reaction center is controlled by the generation of gaseous decomposition product within the reaction center and the mechanical strength of the solid AP in the reactive layer. 5) Reactions cease within the reactive layer when the mechanical strength of the solid AP in the reactive layer can no longer contain the gaseous decomposition products within the reaction centers.

The decomposition processes produce mostly H_2O, O_2, Cl_2, N_2O and HCl, with minor amounts of N_2, NO_2, NO, HClO and a species at *m/z* 69 that contains chlorine (perhaps H_2ClO_2). Minor amounts of NH_3 and $HClO_4$ are also formed from the dissociative sublimation process of AP. The reaction pathways that yield the major products are complex and coupled with the physical processes occurring within the solid AP particles. The fraction of AP that decomposes in the low temperature channel ranges up to approximately 33%, depending upon particle size. The presence of an induction period, the identity of the products, the abrupt appearance and high degree of temporal correlation between the major products, and the decrease in the fraction of AP that decomposes with particle size are strong evidence that the chemical processes occur in the solid phase of the AP particles. These results are similar to those of our earlier work that show the low-temperature decomposition regime of AP in the cubic phase occurs in the solid phase.[7]

The time-dependent behaviors of the formation and evolution rates (GFRs) measured for the product gases show three general features. There is an induction period where very low levels of decomposition gases are detected. The induction period is followed by an acceleratory period where the GFRs of the major products accelerate to simultaneously obtain their maximum value. Then a deceleratory period occurs where the GFRs decay to minimum values. This general behavior of the GFRs is observed for the decomposition of *o*-AP between 171°and 229°C and continues to be general behavior observed when the decomposition of *o*-AP is evaluated as a function of particle size and confinement.

The chemical processes that occur during the induction period involve the nucleation and growth of the reaction centers that form at the subsurface of the AP particles. The confinement of the reaction center allows for the complex chemical interactions to occur that ultimately produce products such as Cl_2, N_2O and the others. The duration of the induction period at a given temperature is not influenced by confinement and particle size. This is consistent with a solid-phase reaction.

The onset of the evolution of decomposition products occur when the reaction centers at the subsurface rupture and the product gases evolve. The formation and destruction of the reaction centers continues to occur as the reaction progresses towards the center of the particle. The highly correlated GFRs of the major product gases is evidence that the product gases are simultaneously evolved from the reaction centers.

FUTURE WORK

The outstanding issues that remain to be addressed will guide our future work.

1. The morphology of the decomposing particle needs to be evaluated in greater detail to fully understand the physical processes. The density of the nucleation sites, the geometry and dimensions of the reaction centers and a mapping of the volume consumed by voids formed as the decomposition propagates through the AP particle will be examined, utilizing SEM and atomic force microscopy.
2. The underlying chemical processes of the thermal decomposition event must be better understood. A global set of reactions and representative kinetics to the reactions must be determined.
3. The temperature dependence of the GFRs of the products needs to be carefully characterized (chemical processes). Data at several temperatures between 170° and 240°C is required to evaluate for trends in the decomposition that may exist at temperatures near phase transition.
4. The effect of high confinement on the reaction must be better understood.
5. Kinetic parameters for the chemical and physical processes will be determined.

ACKNOWLEDGMENTS

The authors thank Mr. Russ Hanush for collecting the mass spectrometry data and Ms. L. Dimeranon for supplying the AP samples. The authors also gratefully acknowledge Alice Atwood and Karl Kraeutle at NAWC for valuable exchanges of information regarding AP decomposition.

REFERENCES

1. Jacobs, P. W. M.; Whitehead, H. M.; *Chemical Reviews* **69**, 551-590 (1969).
2. Bircumshaw, L. L.; Newman, B. H.; *Proceedings of the Royal Society A.* **227**, 115-132 (1954).
3. Bircumshaw, L. L.; Newman, B. H.; *Proccedings of the Royal Society A.* **227**, 228-241 (1954).
4. Manelis, G. B.; Rubtsov, Y. I.; *Russian Journal of Physical Chemistry* **40**; 416-418 (1966).
5. Kraeutle, K. J.; *Third ICRPG Combustion Conference* **138**, pp. 45-50, John F. Kennedy Space Center, NASA, Cocoa Beach, FL: Chemical Propulsion Information Agency (1967).
6. Raevskii, A. V.; Manelis, G. B.; *Proc. Acad. Sci. USSR, Phys. Chem. Sect.* **151**, 686-688 (1963).
7. Behrens, R.; Minier, L.; 1996. *JANNAF Combustion Subcommittee Meeting* **2**, Chemical Propulsion Information Agency, pp. 1-19. Monterey, CA (1996).
8. Jacobs, P. W. M.; Russell-Jones, A.; *AIAA Journal.* **5**, 829 (1967).
9. Behrens, R., Jr.; *Review of Scientific Instruments.* **58**, 451-461 (1987).
10. Behrens, R., Jr.; *International Journal of Chemical Kinetics.* **22**, 135-157 (1990).
11. Behrens, R., Jr.; *International Journal of Chemical Kinetics.* **22**, 159-173 (1990).
12. Kraeutle, K. J.; *Journal of Physical Chemistry.* **74**, 1350-1356 (1970).
13. Solymosi, F.; *Acta Physical Chemistry.* **19**, 67 (1973).
14. Pellett, G. L.; Saunders, A. R.; *Third ICRPG Combustion Conference* **138**, pp. 29-38. John F. Kennedy Space Center, NASA, Cocoa Beach, FL: Chemical Propulsion Information Agency (1967).

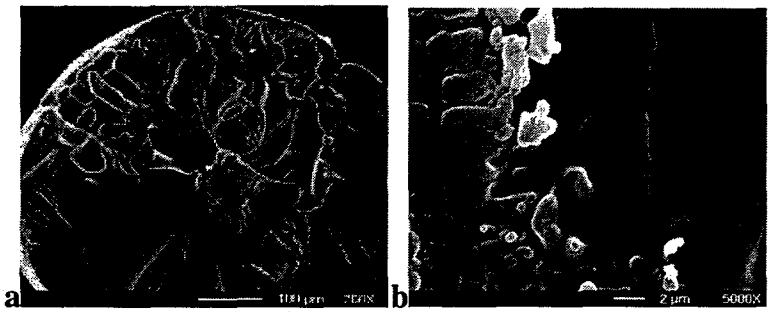

Figure 2. SEM images of the surface of a cleaved, pristine AP particle taken from the nominal 200µm-diameter AP lot (magnification is 200x and 5000x, respectively). The particle shape is spheroidal. Note presence of nonuniform structural defects.

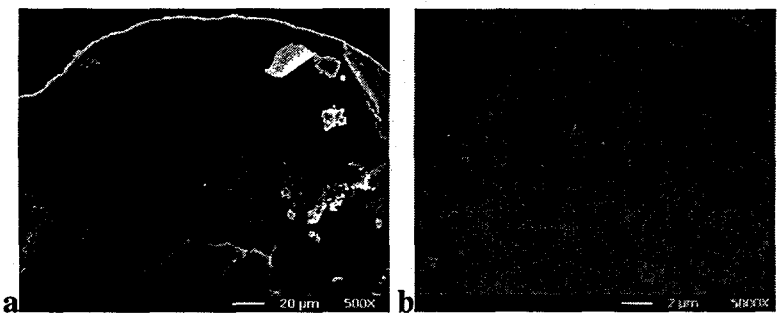

Figure 3. SEM images of a cleaved AP particle held for 2.5 hours at 190°C (magnification is 500x and 5000x, respectively). Approximately 0.5% weight loss due to loss of adsorbed H_2O. No gaseous decomposition products have been released from this particle. Note the increased number of dark regions on the surface. These could be nucleation centers.

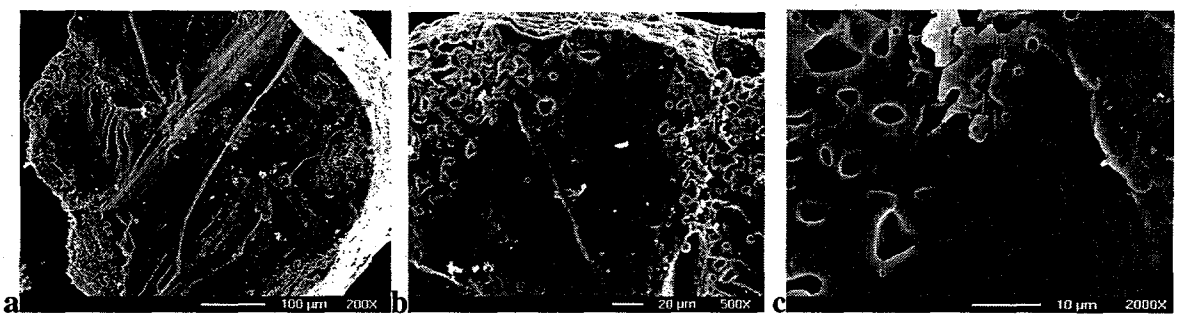

Figure 4. SEM images of a cleaved AP particle held at 190°C for 7.5 hours and losing 3.6% of the sample by weight (magnification is 200x, 500x and 2000x, respectively). Decomposition of particle was stopped during the acceleratory period.

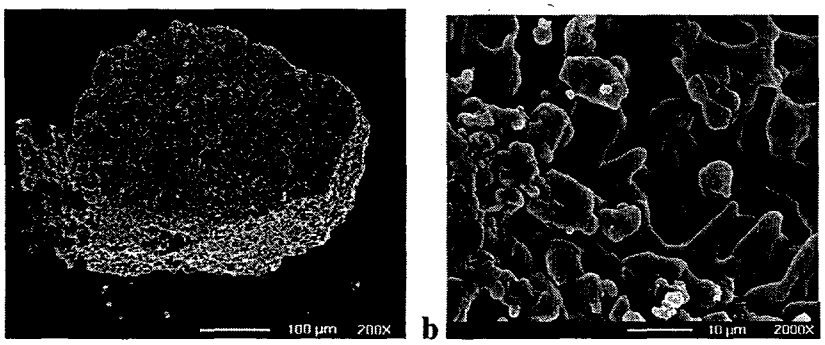

Figure 5. SEM image of a cleaved AP particle held at 192°C for 25 hours (magnification is 200x and 2000x, respectively). Weight loss is 31%. Decomposition is complete. An agglomerate of fine AP remains.

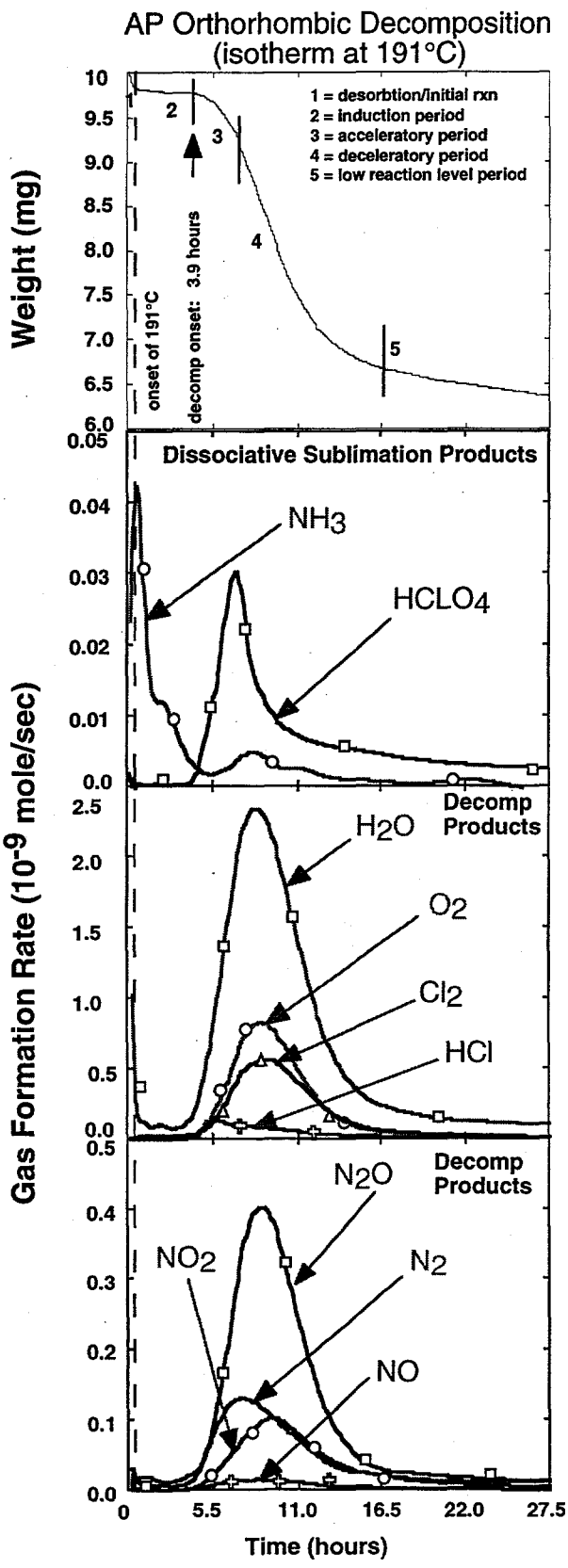

Figure 6. Weight loss profile and gas formation rates for isothermal decomposition of 10.1 mg neat AP (nominal 200μm) at 191°C. The reaction cell orifice diameter is 25μm.

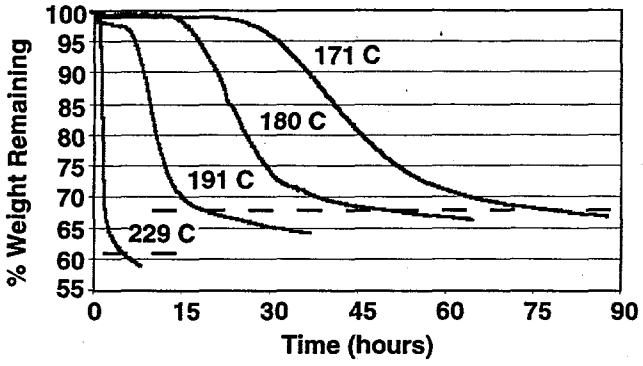

Figure 7. Percent weight loss profiles for orthorhombic AP as a function of temperature. Isothermal decompositions were conducted on ~10 mg AP in a reaction cell fitted with a 25μm-diameter orifice. Dashed lines indicate the end of the major decomposition event.

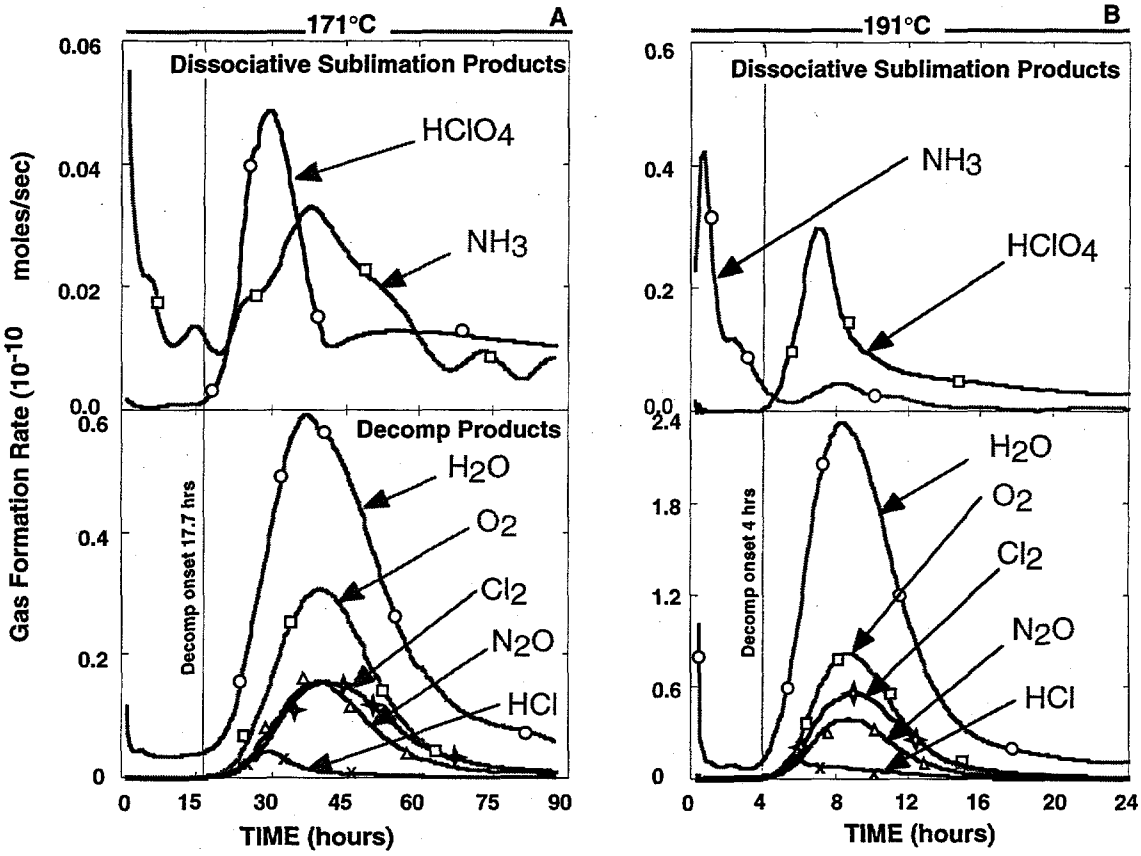

Figure 8. Temporal behavior of the GFRs of the products resulting from the isothermal decomposition of orthorhombic AP at the isothermal temperatures of 171°C and 191°C. A sample of ~10mg of the nominal 200μm-diameter AP is used in each experiment. The reaction cell is fit with a 25μm-diameter orifice.

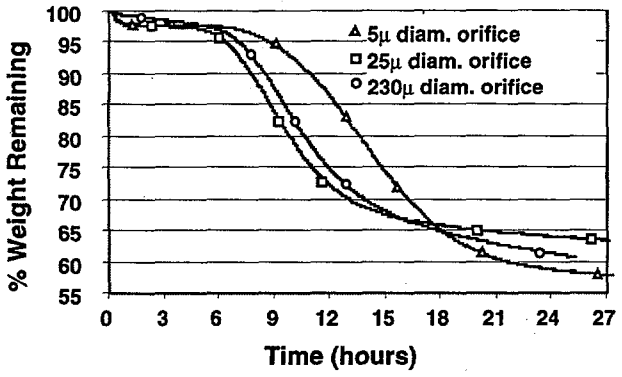

Figure 9. Percent weight loss profiles for orthorhombic AP as a function of orifice diameter. Isothermal decompositions were conducted on ~10 mg samples of AP in a reaction cells fitted with a 5μm, 25μm and 230μm-diameter orifices, respectively.

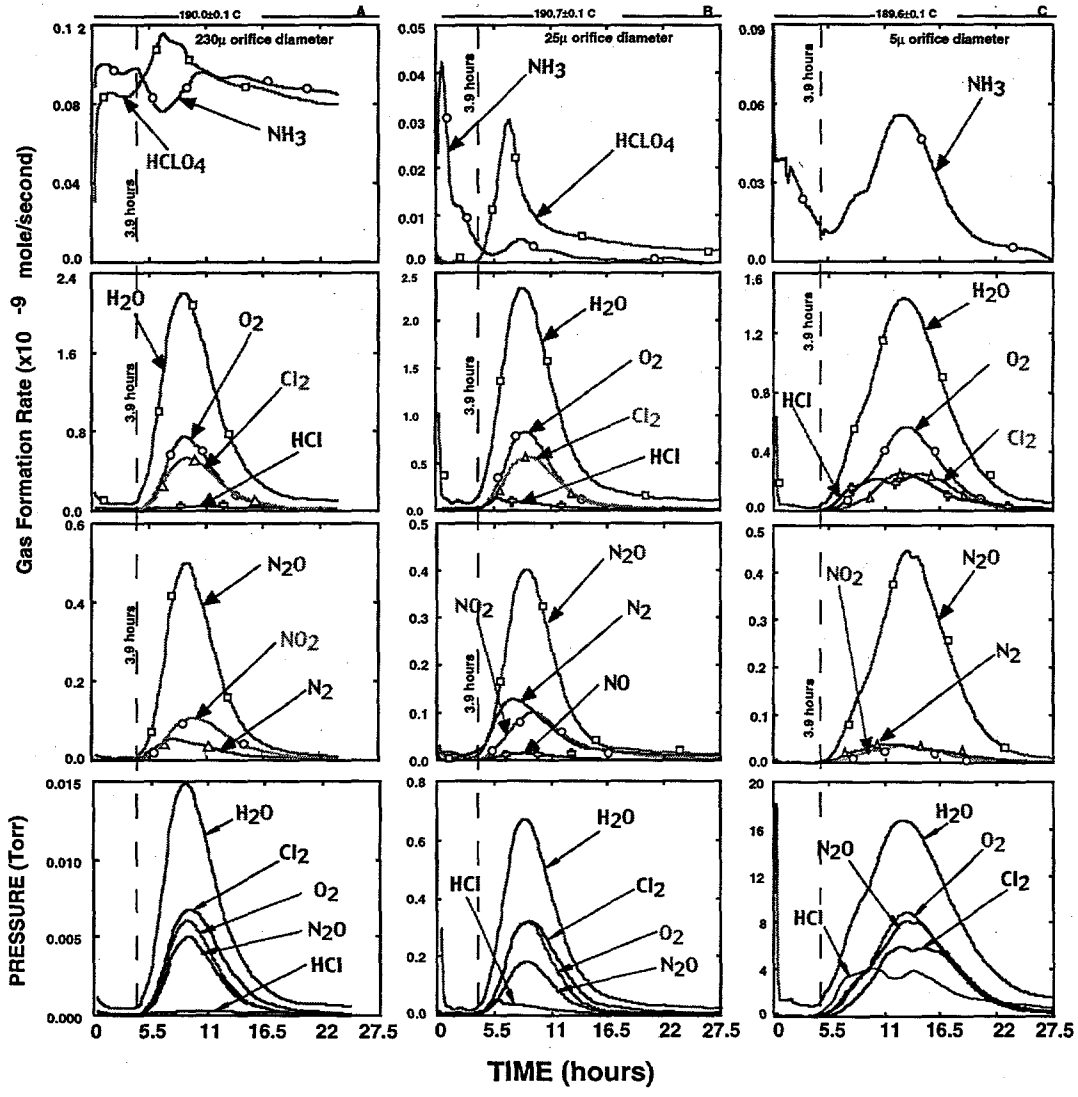

Figure 10. Temporal behaviors of theGFRs, and the corrresponding partial pressures of the decomposition products within the reaction cell, for three different reaction cell orifice diameters. Products not included in the analysis due to their low ion signals are NO (columns A and C) and $HClO_4$ (column C).

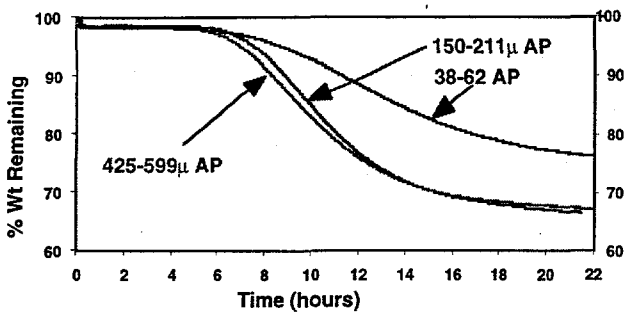

Figure 11. Characteristic weight loss profiles for AP particles from three different particle-size distributions. The narrow distributions were obtained as fractions from the seiving of the nominal 200μm-diameter AP lot.

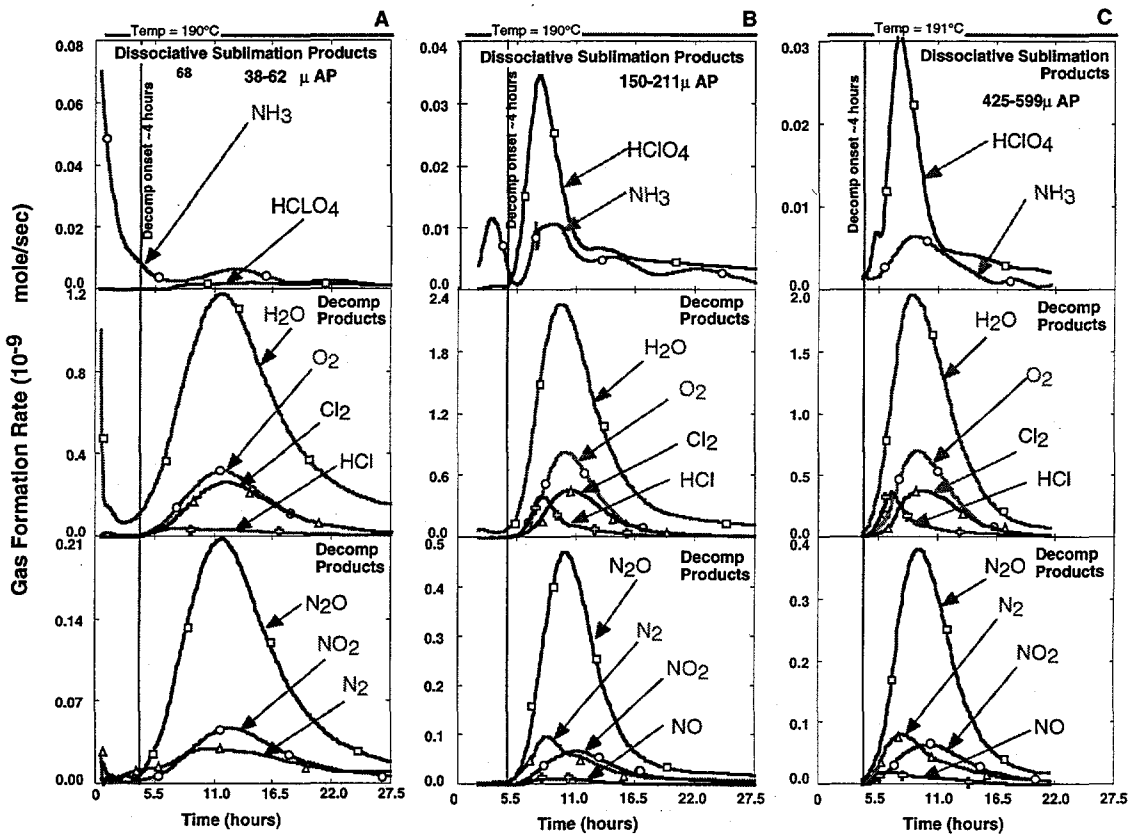

Figure 12. Temporal behavior of the gaseous products resulting from the isothermal decomposition of neat AP at ~190°C for three different AP particle size distributions: 38-62μm AP (A), 150-211μm AP (B), and 425-599μm AP (C). The reaction cell is fitted with a 25μm-diameter orifice for all three experiments. The time until onset of decomposition is independent of the AP particle size. The NO product is not included in the 38-62μm AP due to the low level of the original ion signal of NO in the mass spectral data, thus making it difficult to add in the analysis.